

## ОБЩАЯ И ФИЗИЧЕСКАЯ ХИМИЯ

UDC 546.786:546.742:546.06

### REACTION PATHWAY IN THE WO<sub>3</sub>-NiO-Mg-C SYSTEM. DTA/TG STUDY

M. K. ZAKARYAN<sup>1,2</sup>, O. M. NIAZYAN<sup>1</sup>, S. V. AYDINYAN<sup>1,3</sup> and S. L. KHARATYAN<sup>1,2</sup>

<sup>1</sup>A.B. Nalbandyan Institute of Chemical Physics NAS RA  
5/2, P. Sevak Str., Yerevan, 0014, Armenia

<sup>2</sup>Yerevan State University

1, A. Manoukyan Str., Yerevan, 0025, Armenia

<sup>3</sup>Tallinn University of Technology

5, Ehitajate tee, Tallinn, 19086, Estonia

E-mail: zakaryan526219@gmail.com

The reaction pathway for the joint reduction of nickel and tungsten oxides with the use of Mg/C combined reducer was studied by DTA/TG technique. It was revealed that reduction of the metal oxides is initiated with double-stage magnesiothermal reduction (reducing the nickel oxide, firstly, and tungsten oxide, secondly) at temperatures near the melting point of magnesium. The carbothermal reduction process started later. Then at 900 °C MgWO<sub>4</sub> salt formation occurs by the interaction of unreduced tungsten oxide with the formed magnesium oxide. According to the data obtained, the heating rate essentially affects stepwise nature of the process. With decreasing the heating rate the magnesiothermal reduction stages were completely splitted.

Figs. 8, references 23.

## 1. Introduction

Tungsten is an ideal choice in space vehicles and fourth generation nuclear reactor applications [1,2]. However, tungsten applications are limited due to high ductile-brittle transition temperature. Nickel addition modifies the core of dislocation which results in reduction of Peierls stress and enhances the ductility. Moreover, Ni addition facilitates liquid phase sintering to improve densification owing to lower melting point [3-6]. Thanks to that, W-Ni alloys have been adopted for many engineering applications due to their excellent physicochemical properties. High mechanical strength, high Young's modulus, low thermal expansion, good

ductility, excellent resistance to corrosion and radiation, as well as good formability and non-radiation pollution render their performance as mass balance, radiation shielding, corrosion and wear-resistant materials and attractive candidates for using as kinetic energy penetrators to replace the depleted uranium alloys [7,8]. W-Ni alloys are usually fabricated by conventional powder metallurgy (PM), however it consumes too much sintering time and energy and mechanical properties are low due to the coarse grain microstructure of tungsten [9]. Therefore, recent reports illustrate the need of new synthesis technologies to reduce grain size and refine microstructure to improve mechanical properties [10-13]. Energy-saving self-propagating high-temperature synthesis (SHS) or combustion synthesis (CS) provides a technological advance for the synthesis of metal powders, alloys and nanocomposites of high purity in a controllable thermal regime. Due to the application of reactions coupling approach the reduction of metal oxides can be performed at relatively low temperature mode using Mg+C combined reducers [14-16].

However, considering that combustion processes are characterized by high temperatures and high self-heating rates of substances in the combustion front, considerable difficulties arise for exploring the interaction mechanism of the combustion process and optimizing synthesis conditions. Thermal analysis is a very powerful method ranging from exploring interaction mechanism to optimizing synthesis conditions and testing materials properties.

According to the available literature data, the mechanism and kinetics of reduction of separate oxides of tungsten and nickel was recently explored [17,18]. It was revealed that the reduction of nickel (II) oxide with simultaneous utilization of Mg and C is initiated by Mg, followed by simultaneous action of magnesium and carbon, and at the end of the magnesiothermal process the second stage of the carbothermal reduction started leading to the formation of nickel powder. It was established that utilization of Mg/C combined reducer allows to mitigate the reduction temperature of NiO and to decrease the activation energy values compared to the separate carbothermal and magnesiothermal reduction reactions due to the synergistic effect of combined reducers. In the  $WO_3$ -Mg-C ternary system [18] the reduction starts with solid Mg, then continues with stepwise carbothermal reduction of tungsten oxides, and the reduction temperature is shifted to higher temperature range compared to separate magnesiothermal reduction process. However in all cases the reduction completes before temperature reaches melting point of Mg.

The combined reduction of two metals is also of considerable practical interest, since it is precisely the joint reduction of Ni and W that allows to obtain Ni-W composites/alloys with a more uniform microstructure. Thus, co-reduction of  $WO_3$  and NiO oxides with the help of the combined reducing

agent Mg/C is the main task considered in this study. XRD analysis of the quenched products together with the kinetic data of the reduction processes at various stages were used to elucidate the reduction mechanism under non-isothermal conditions by the DTA/TG method.

## 2. Materials and methods

The experiments were carried out by differential thermal (DTA) and thermogravimetric (TG) analysis methods using Q-1500 instrument (Derivatograph Q1500 MOM, Hungary). The reactive powder mixture (80-200 mg) was placed into one of two crucibles. In the second crucible the  $\text{Al}_2\text{O}_3$  powder was placed, which is used as a reference material. All measurements were conducted in nitrogen flow ( $100\text{-}120\text{ ml}\cdot\text{min}^{-1}$ ). Heating rate was programmed to be 2.5, 5, 10,  $20^\circ\text{C}\cdot\text{min}^{-1}$ .

As raw materials nickel (II) oxide (reagent grade, Russia, TU 6-09-4125-80), tungsten (VI) oxide (Pobedit Company, Russia, pure, high grade,  $\mu < 40\ \mu\text{m}$ ), magnesium (MPF-3, Russia, pure, particle size  $0.15\text{ mm} < \mu < 0.3\text{ mm}$ ) and carbon (P-803, Russia,  $\mu < 0.1\ \mu\text{m}$ ) were used in experiments.

## 3. Results and discussion

For better understanding of the reaction mechanism in the NiO- $\text{WO}_3$ -Mg-C quaternary system, firstly ternary systems ((NiO- $\text{WO}_3$ -Mg), (NiO- $\text{WO}_3$ -C)) were explored in the same conditions taking into account the results obtained earlier for the binary (NiO-Mg, NiO-C,  $\text{WO}_3$ -Mg,  $\text{WO}_3$ -C) and ternary (NiO-Mg-C,  $\text{WO}_3$ -Mg-C) systems [17,18].

### 3.1. NiO- $\text{WO}_3$ -Mg ternary system

Figure 1 depicts DTA curve for the NiO+ $\text{WO}_3$ +4Mg stoichiometric mixture. As it can be seen, there are two peaks on the DTA curve ( $T_{\text{max}} = 595, 645^\circ\text{C}$ ), which correspond to the exothermic reductions of the two oxides (Fig. 1).

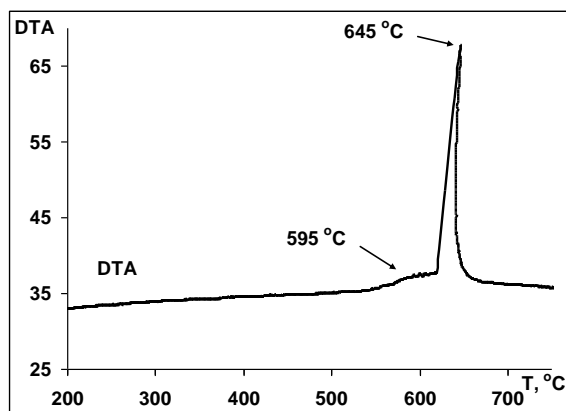


Fig. 1. DTA curve of the NiO+ $\text{WO}_3$ +4Mg mixture,  $V_h = 10\ ^\circ\text{C}\cdot\text{min}^{-1}$ ,  $m_o = 80\text{ mg}$ .

The first, weak peak appeared before Mg melting, illustrates the reduction of oxide with a solid + solid mechanism. Unlike the latter, the second reduction stage includes the reducer's melting range.

In order to explore the interaction mechanism and particularly, find out which oxide interacts with magnesium firstly, the heating was interrupted and XRD examinations were performed respectively. The sample cooled down from temperature 605°C besides initial reagents contains small amount of reduced nickel (Fig. 2). XRD pattern of the sample cooled down from 690°C, contain also characteristic peaks of reduced tungsten. At higher temperatures (910°C), the NiO and WO<sub>3</sub> are absent, however apart from the target metals and magnesium oxide, magnesium tungstate, MgWO<sub>4</sub> was also registered (Fig. 2). Thus, according to the data obtained, sequential reduction of oxides occurs: at the first stage the magnesiothermal reduction of nickel oxide takes place, followed by the joint reduction of both oxides. At higher temperatures the MgWO<sub>4</sub> formation occurs by the interaction of unreduced tungsten oxide with the formed magnesium oxide.

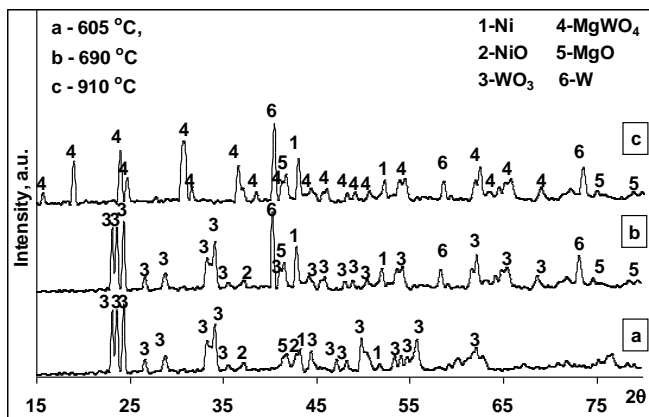


Fig. 2. XRD patterns of the NiO+WO<sub>3</sub>+4Mg reaction products cooled down from different characteristic temperatures.

Comparing the obtained data with those for magnesiothermal reduction of individual oxides, it becomes clear that in the case of joint reduction of oxides, the sequence of reduction processes changes. Thus, according to [17,18] the magnesiothermal reduction of tungsten oxide took place at a lower temperature (581°C) compared with the reduction of nickel oxide (664°C) by 80-85°C.

### 3.2. NiO-WO<sub>3</sub>-C ternary system

In the figure 3 the DTG curves for NiO+WO<sub>3</sub>+4C and 3NiO+WO<sub>3</sub>+4C mixture are shown. These attempts allowed to record two adjacent stages of reduction processes on DTG curves. It was expected that the increase in the NiO amount in the initial mixture will be expressed with more defined signal on the DTG curve. Indeed, the increase of the amount of nickel oxide allows

comprehending that the first stage is the carbothermal reduction of nickel oxide, followed by the reduction of tungsten oxide. The conclusion is based on the fact that when increasing the amount of NiO, spreading of the DTG minimum within 825-920°C temperature range increases (Fig. 3) which corresponds to the nickel oxide reduction area. The latter was followed by the tungsten oxide reduction process (at 925°C).

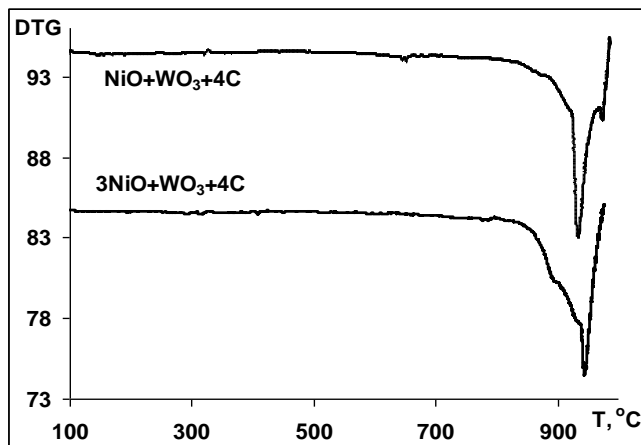


Fig. 3. DTG curves of the NiO+WO<sub>3</sub>+4C, 3NiO+WO<sub>3</sub>+4C mixtures,  $V_h = 20^\circ\text{C}\cdot\text{min}^{-1}$ ,  $m_o = 200\text{ mg}$ .

Thus, by the introduction of tungsten oxide into NiO-C system, the reduction of nickel oxide shifts to the higher temperature area (Fig. 4) as registered in [18]. However, unlike magnesiothermal reduction of two oxides, exchange of positions of reduction processes (in terms of sequence) does not occur [17,18].

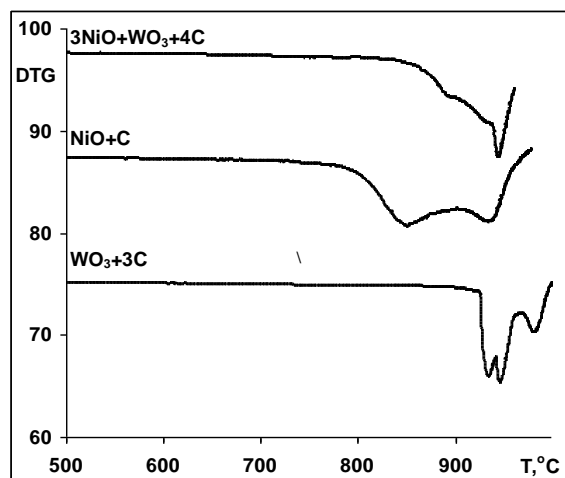


Fig. 4. DTG curves of the NiO+WO<sub>3</sub>+4C, NiO+C, WO<sub>3</sub>+3C mixtures,  $V_h = 20^\circ\text{C}\cdot\text{min}^{-1}$ ,  $m_o = 200\text{ mg}$ .

According to XRD analysis results obtained for the products of the NiO+WO<sub>3</sub>+4C mixture quenched at 960°C, nickel and tungsten oxides interact at high temperatures with formation of nickel tungstate, NiWO<sub>4</sub>, (Fig. 5). Thus, instead of full carbothermal reduction, the formation of nickel tungstate took place. It means that the reaction of salt formation proceeds earlier/faster than carbothermal reduction, therefore nickel tungstate reduction would take place at higher temperatures.

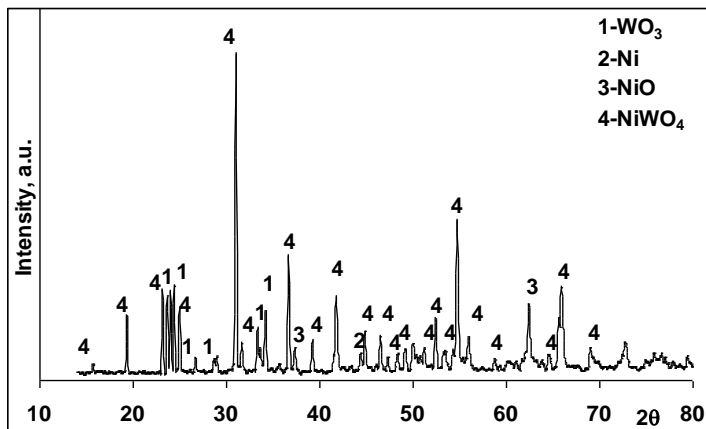


Fig. 5. XRD pattern of the NiO+WO<sub>3</sub>+4C reaction product, T = 960°C, V<sub>h</sub> = 20°C·min<sup>-1</sup>.

### 3.3. NiO-WO<sub>3</sub>-Mg-C quaternary system

The kinetics and mechanism of combined reduction process of metal oxides have been investigated from different points of view. It was found that the reduction process of metal oxide mixtures is mainly characterized by a stepwise course of reaction. As usual, the initial reduction of thermodynamically less stable metal oxides facilitates the reduction of the others [19-21]. As an example, according to the [19] in the WO<sub>3</sub>/CuO system the formation of metallic copper clearly accelerates the reduction of WO<sub>3</sub>.

As can be seen from the DTA/TG/DTG curves for the NiO+WO<sub>3</sub>+Mg+2C quaternary mixture (Fig. 6) the process was initiated with double-stage magnesiothermal reduction (with T<sub>max</sub> at 615 and 660°C). The endothermic stage observed on the DTA curve at 645-650°C corresponds to the magnesium melting. It can be concluded from the behavior of TG/DTG curves (Fig. 6), that the decrease in the mixture's mass started after the magnesiothermal reduction (DTG<sub>min</sub> = 927°C).

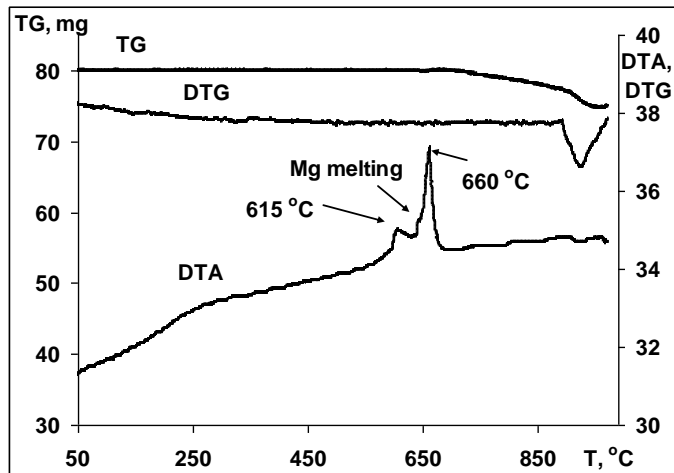


Fig. 6. DTA/TG/DTG curves of the NiO+WO<sub>3</sub>+Mg+2C mixture,  $V_h = 5 \text{ }^\circ\text{min}^{-1}$ ,  $m_0 = 80 \text{ mg}$ .

To find out the priority of reactions, the process has been interrupted at 630 and 700°C (after two magnesiothermal stages). The samples cooled down from different temperatures were exposed to XRD examinations.

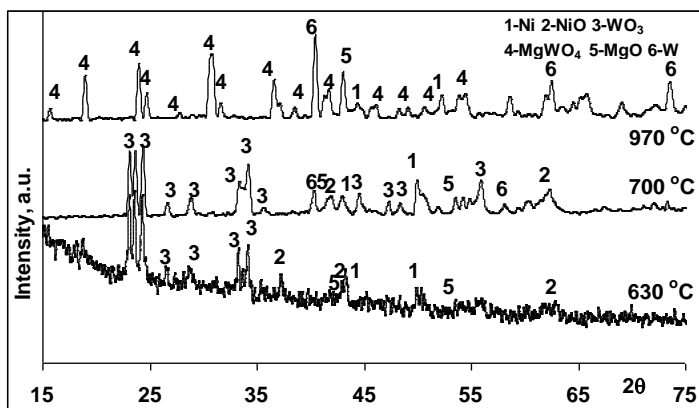


Fig. 7. XRD patterns of the NiO+WO<sub>3</sub>+Mg+2C reaction products cooled down from different temperatures.

According to the results obtained, the sample cooled down from 630°C contains tungsten oxide, nickel oxide, magnesium oxide and reduced nickel. In the sample cooled down from 700°C reduced tungsten was also observed. When the temperature reaches 970°C, the MgWO<sub>4</sub> formation process begins (Fig.7). Besides, presumably based on the TG/DTG curves (Fig. 6), carbon began to participate in the reduction process. It can be concluded, that the reduction process starts by magnesium reduction of the nickel oxide, firstly, and tungsten oxide, secondly. Later, the reduction process was continued by carbon that reacts with the rest oxides. At much higher temperatures the MgWO<sub>4</sub> salt formation took place.

The examinations for the  $\text{NiO}+\text{WO}_3+\text{Mg}+2\text{C}$  mixture were performed at various heating rates for exploring influence of the heating rate on the reaction pathway. As can be seen (Fig. 8) the heating rate essentially affects the expression of the stepwise nature of the process. With decreasing of the heating rate the exothermic magnesiothermal reduction stages were splitted completely. In the case of  $20^\circ\cdot\text{min}^{-1}$  heating rate, the stages are completely overlapped (Fig. 8).

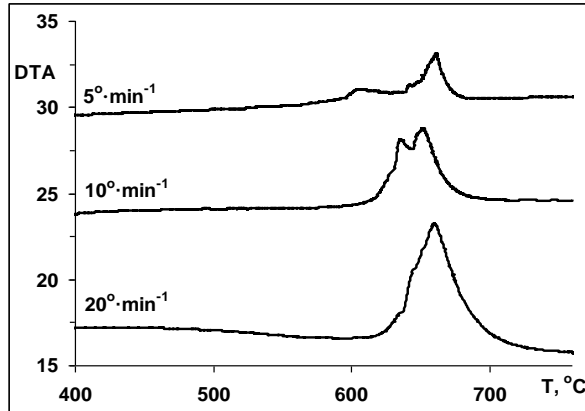


Fig. 8. DTA curves of the  $\text{NiO}+\text{WO}_3+\text{Mg}+2\text{C}$  mixture at various heating rates.

### 3.4. $\text{NiWO}_4\text{-Mg-C}$ system

The series of experiments were carried out for the  $\text{NiWO}_4\text{-Mg-C}$  system too, for clarifying the difference between the mechanisms of the oxides and salt reduction processes. Some outcomes could be enumerated from the examinations: (i) magnesiothermal reduction of the initial salt  $\text{NiWO}_4$  starts before magnesium melting, (ii) addition of carbon leads to the shift of magnesiothermal reduction to higher temperatures and the reduction starts by molten magnesium, (iii) carbothermal reduction process doesn't proceed in the given temperature range and in the presence of carbon further reduction process is inhibited. It is worthy to note that magnesio-carbothermal reduction process for this system is completely different from those for the  $\text{CuMoO}_4$  and  $\text{CuWO}_4$  [22-23]. Unlike those, in this case the potential temperature domain of the used device is not enough for complete reduction of both metals from the initial  $\text{NiWO}_4$ .

### ՓՈՒՍԱԶԳԵՅՈՒԹՅԱՆ ՄԵԽԱՆԵՐԻ ՉՄԱՆՈՒՄԸ $\text{WO}_3\text{-NiO-Mg-C}$ ՆԱՄԱԿԱՐԳՈՒՄ. ԴԵՐԻՎԱՏՈԳՐԱՖԻԱԿԱՆ ՈՒՄՈՒՄՆԱՍԻՐՈՒԹՅՈՒՆ

Մ. Կ. ԶԱԲԱՐՅԱՆ, Օ. Մ. ՆԻԱԶՅԱՆ, Ս. Վ. ԱՅԻՆՆՅԱՆ և Ս. Լ. ԽԱՌԱՏՅԱՆ

Ուսումնասիրվել է  $\text{NiO}$  և  $\text{WO}_3$  օքսիդների համատեղ վերականգնման մեխանիզմը  $\text{Mg/C}$  համակցված վերականգնիչով գծային տաքացման պայմաններում: Բացահայտվել է, որ պրոցեսն սկսվում է մետաղների օքսիդների երկփուլ մագնեթիումաթերմ վերա-

կանգնմամբ (սկզբում նիկելի օքսիդի, այնուհետև՝ վոլֆրամի օքսիդի): Կարբոթերմ վերականգնման պրոցեսն ընթանում է ավելի բարձր ջերմաստիճաններում: Ջերմաստիճանի հետագա բարձրացումն ուղեկցվում է նաև  $MgWO_4$  աղի առաջացմամբ: Ստացված սվյալների համաձայն, տաքացման արագությունը զգալիորեն ազդում է պրոցեսի փուլային բնույթի դրսևորման վրա, մասնավորապես, տաքացման արագության նվազմանը զուգընթաց Հնարավոր է դառնում ամբողջովին բաժանել երկու օքսիդների մագնիզիում-մաթերմ վերականգնման էկզոթերմ փուլերը:

## DTA/TG ИССЛЕДОВАНИЕ МЕХАНИЗМА РЕАКЦИИ В СИСТЕМЕ $WO_3$ -NiO-Mg-C

М. К. ЗАКАРЯН<sup>1,2</sup>, О. М. НИАЗЯН<sup>1</sup>, С. В. АЙДИНЯН<sup>1,3</sup> и С. Л. ХАРАТЯН<sup>1,2</sup>

<sup>1</sup>Институт химической физики им. А.Б. Налбандяна НАН Республики Армения

Армения, 0014, Ереван, ул. П. Севака, 5/2

<sup>2</sup>Ереванский государственный университет

Армения, 0025, Ереван, ул. А. Манукяна, 1

<sup>3</sup>Таллинский технологический университет

Эитайате ул. 5, Таллинн, 19086, Эстония

E-mail: zakaryan526219@gmail.com

Исследован механизм восстановления оксидов NiO и  $WO_3$  комбинированным восстановителем Mg/C в условиях линейного нагрева. Установлено, что процесс начинается двухстадийным магниотермическим восстановлением металлов (сначала оксида никеля, затем оксида вольфрама). Карботермическое восстановление протекает при более высоких температурах. При этом наблюдается также образование соли  $MgWO_4$ . Согласно полученным данным, скорость нагрева существенно влияет на проявление ступенчатой природы процесса восстановления. В частности, с уменьшением скорости нагрева экзотермические стадии магниотермического восстановления полностью разделяются.

## REFERENCES

- [1] Rieth M., Dudarev S.L., Gonzalez de Vicente S.M., Aktaa J., Ahlgren T. // J. Nucl. Mater., 2013, v. 432, №1-3, p. 482.
- [2] Chechenin N.G., Chuvilskaya T.V., Shirokova A.A., Kadenskii A.G. // Phys Atom Nucl, 2015, v. 78, №1, p. 159.
- [3] Wurster S., Baluc N., Battabyal M., Crosby T., Du J., Garcia-Rosales C., Hasegawa A., Hoffmann A., Kimura A., Kurishita H., Kurtz R.J., Li H., Noh S., Reiser J., Riesch J., Rieth M., Setyawan W., Walter M., You J.H., Pippan R. // J. Nucl. Mater., 2013, v. 442, №1-3, p. S181.
- [4] Kemp P.B., German R.M. // J. Less Common Met., 1991, v. 175, №2, p. 353.
- [5] Patra A., Saxena R., Karak S.K., Laha T., Sahoo S.K. // J. Alloy. Compd., 2017, v. 707, p. 245.
- [6] Talekar V.R., Patra A., Sahoo S.K., Karak S.K., Mishra B. // Int. J. Refract. Met. H., 2019, v. 82, p. 183.
- [7] Donten M., Henrikas C., Zbigniew S. // Electrochim. Acta, 2000, v. 45, №20, p. 3389.
- [8] Królikowski A., Płońska E., Ostrowski A., Donten M., Stojek Z. // J. Solid State Electr., 2019, v. 13, №2, p. 263.
- [9] Bhattacharjee P.P., Ray R.K., Upadhyaya A. // Scripta Mater., 2005, v. 53, №12, p. 1477.

- [10] *Al-Kelesh H., Abdel Halim K.S, Nasr M.I.* // *J. Mater. Res.*, 2019, v. 31, №19, p. 2977.
- [11] *Shu-dong L., Jian-hong Y., Ying-Li G., Yuan-dong P., Li-ya L., Jun-ming R.* // *J. Alloy. Compd.*, 2009, v. 473, №1-2, p. L5.
- [12] *Fan J.L., Liu T., Cheng H., Wang D.* // *J. Mater. Process. Technol.*, 2008, v. 208, p. 463.
- [13] *Elias L., Scott K., Hegde A.Ch.* // *J. Mater. Eng. Perform.*, 2015, v. 24, №11, p. 4182.
- [14] *Aydinyan S.V., Kirakosyan H.V., Zakaryan M.K., Abovyan L.S., Kharatyan S.L., Peikrishvili A., Mammiashvili G., Godibadze B., Chagelishvili E.Sh., D.R. Lesuer, Gutierrez M.* // *Eurasian Chem.-Technol. J.*, 2018, v. 20, №4, p. 301.
- [15] *Kirakosyan H.V., Aydinyan S.V., Kharatyan S.L.* // *Int. J. SHS*, 2016, v. 25, №4, p. 215.
- [16] *Zakaryan, M., Kirakodyan H., Aydinyan S., Kharatyan S.* // *Int. J. Refract. Met. H.*, 2017, v. 64, p. 176.
- [17] *Zakaryan M.K., Niazyan O.M., Aydinyan S.V., Kharatyan S.L.* // *Arm. Chem. J.*, 2018, v.71, №4, p. 473.
- [18] *Baghdasaryan A.M., Niazyan O.M., Khachatryan H.L., Kharatyan S.L.* // *Int. J. Refract. Met. H.*, 2014, v. 43, p. 216.
- [19] *Aydinyan S., Kirakosyan H., Niazyan O., Tumanyan M., Nazaretyan Kh., Kharatyan S.* // *Arm. J. Phys.*, 2016, v. 9, №1, p. 83.
- [20] *Kirakosyan H., Minasyan T., Niazyan O., Aydinyan S., Kharatyan S.* // *J. Therm. Anal. Calorim.*, 2016, v. 123, №1, p. 35.
- [21] *Aydinyan S., Nazaretyan Kh., Zargaryan A, Tumanyan M., Kharatyan S.* // *J. Therm. Anal. Calorim.*, 2018, v. 133, №1, p. 261.
- [22] *Aydinyan S.V., Kirakosyan H.V., Niazyan O.M., Kharatyan S.L.* // *Arm. Chem. J.*, 2015, v.68, №2, p. 196.
- [23] *Aydinyan S.V., Kirakosyan H.V., Tumanyan M., Kharatyan S.L* // Abstract of the IV International Conference "Current Problems of Chemical Physics", Yerevan, 5-9 October, 2015, p.143.